

Research Article

Open Access

Raid Ramzi Al-Omari, Madhat Shakir Al-Soud*, Osamah Ibrahim Al-Zuhairi

Effect of Tunnel Progress on the Settlement of Existing Piled Foundation

<https://doi.org/10.2478/sgem-2019-0008>

received July 18, 2018; accepted February 13, 2019.

Abstract: Tunnel construction below or adjacent to piles will affect the performance and eventually the stability of piles due to ground deformation resulting in the movement of piles and changes in the axial force distribution along the piles. A three dimensional finite element analysis using PLAXIS 3D (2013) was performed to study the behaviour of a single pile and 3 x 3 piles group during the advancement of shield tunnelling in ground. The 10-node tetrahedral elements were used to model both the soil and the tunnel lining. The Hardening Soil (HS) model was used to simulate the soil structure interaction at the tunnel-soil interface. An isotropic elastic model was used for the pile, piles cap, tunnel lining and tunnel boring machine shield (TBM). Several parametric studies were attempted including the longitudinal, lateral, and vertical tunnel location relative to pile embedded in different types of soil (clay or sand). The results showed that the pile head settlement increases during the tunnelling advancement in larger values than that for ground surface settlement. A zone of influence was determined in the range of twice the tunnel diameter in the longitudinal direction (forward and backward of the pile), and transverse direction (left and right of the tunnel centreline). If the tunnel boring is kept off this zone then there is no fear of pile collapse.

Keywords: Numerical modelling and analysis; piles; soil-structure interaction; tunnelling.

1 Introduction

Tunnelling has been widely used during the past decades. Due to the fast population growth and industrial activity, such type of infrastructures becomes a common technique in the urban area providing a wide range of facilities (transportation, electric line, ditches, etc...). For high-rise buildings supported by deep foundations, the construction of tunnel induces ground movements, which in turn affect the bearing capacity as well as the settlement of the existing piles.

There has been considerable research examining the behaviour of the soil-tunnel-pile interaction and the possible damage on an existing piled foundations caused by tunnelling. These include field observations (Mair 1993; Forth and Thorley 1996), geotechnical centrifuge modelling (Loganathan et al. 2000; Jacobsz et al. 2002; Ng et al. 2013, Mair and Williamson 2014, Boonsiri and Takemura 2015) and analytical and numerical modelling (Lee and Ng 2006; Lee et al 2007, Yang et al 2011, Miro et al 2011, Fattah et al 2014, Lee 2012, Lee 2013, Yoo 2013, Basile 2014, Lee et al 2016).

The objective of this study is to investigate the behaviour of piled foundation due to tunnel construction. The main aims of the study are to numerically estimate the longitudinal, lateral, and vertical distances of the tunnel face from piles after which further tunnelling progress would be risky.

2 Finite Element Modelling

2.1 Discretization and Boundary Conditions

Single and group of (3 × 3) piles with an optimum centre-to-centre spacing of $s = 3d$ (Bowles, 1997) were modelled to study the behaviour of the pile groups, where d is the diameter of the pile and D is the diameter of the tunnel. Figure 1 shows the three dimensional finite element mesh that was used in the numerical analyses. The mesh

*Corresponding author: Madhat Shakir Al-Soud: Mustansiriya University, College of Engineering, E-mail: ms_madhat@uomustansiriya.edu.iq

Raid Ramzi Al-Omari: Al- Farabi University College, Civil Engineering Department

Osamah Ibrahim Al-Zuhairi: Al- Nahrain University, College of Engineering

dimensions in the x-direction are 60 m (10 D), that is, 30 m in each side of the centre line of the tunnel, y-direction is 81 m (13.5 D), and in the z-direction is 36 m (6 D). The mesh consists of nearly 28,000 elements (10-node tetrahedrons) with over 32,000 nodes. The boundary conditions of the geometry model are as given below:

- Vertical model boundaries with their normal in x-direction (i.e., parallel to the y_z -plane) are fixed in the x-direction ($u_x = 0$) and free in y- and z-direction.
- Vertical model boundaries with their normal in y-direction (i.e., parallel to the x_z -plane) are fixed in the y-direction ($u_y = 0$) and free in x- and z-directions.
- Vertical model boundaries with their normal neither in x- nor in the y-direction are fixed in x- and y-directions ($u_x = u_y = 0$) and free in z-direction.
- The model bottom boundary is fixed in all directions ($u_x = u_y = u_z = 0$).
- The ‘ground surface’ is free in all directions.

A fine mesh was used near the tunnel and pile locations due to the concentration of large shear strains; while a coarser mesh was used outside these zones. The tunnel diameter D is constant throughout the analysis and is equal to 6 m. Figure 2 shows the sectional views of the geometry used in the analysis for a single pile and group of piles, respectively, where E is the lateral distance from the tunnel centre to the pile centre in case of single pile analysis and to the pile group centre in case of pile group analysis, and C is the vertical clearance between the pile tip and the tunnel crown. The pile’s length (L_p) was assumed to be 18 m with a diameter (d) of 1 m. The connection of piles with the cap was assumed to be a hinge, and the thickness of the pile cap is 1 m. In this study, the behaviour of the centre and corner piles within the pile group was analysed. The pile cap dimensions and the positions of the piles within the group are shown in Figure 3. It is assumed that the construction was performed using the shield tunnelling tunnel boring machine (TBM) (Chapman, 2010). The water table level was assumed to be at the ground surface and the hydrostatic pore pressure was kept constant during the tunnel boring advancement.

2.2 Material Parameters and Constitutive Models

An elasto-plastic analysis was adopted to simulate tunnel construction. Pile–soil interaction was included using the embedded pile feature (Brinkgreve et al., 2013). The embedded pile is a pile composed of beam elements that can be placed in an arbitrary direction in the sub-soil

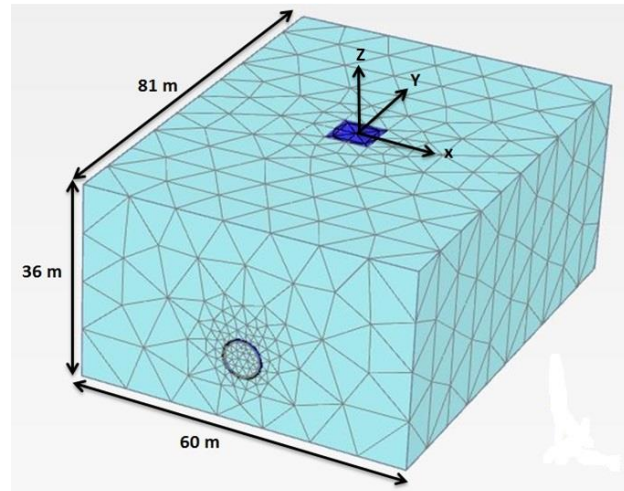


Figure 1: 3D finite element meshes, dimensions of problem and axis location used in the analysis.

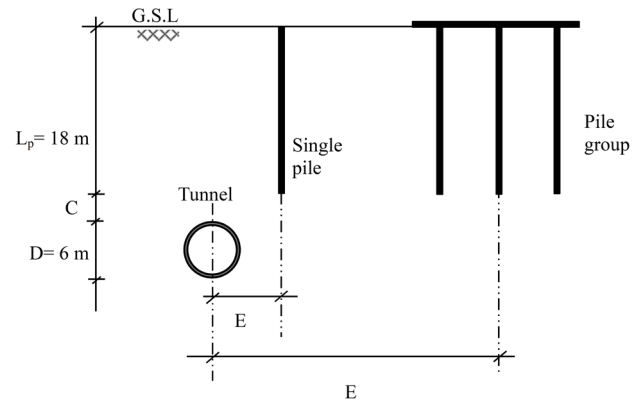


Figure 2: Underground location of tunnel relative to a single and group of piles.

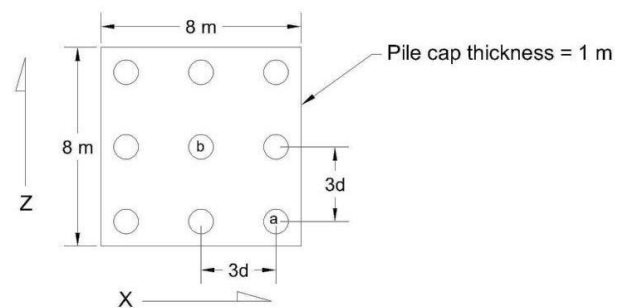


Figure 3: Piles cap dimension and Locations of piles in groups.

and that interacts with the sub-soil by means of special interface elements.

Table 1: Concrete parameters adopted in the numerical analysis.

Parameters	Values				Units	Model
	Pile	Pile cap	Tunnel lining	TBM shield		
Diameter (D)	1	-	-	-	m	Linear elastic
Thickness (t)	-	1	0.25	0.35	m	
Elasticity modulus (E)	30×10^6	30×10^6	30×10^6	210×10^6	kN/m^2	
Unit weight (γ)	25	25	25	38	kN/m^3	
Poisson's ratio (ν)	0.2	0.2	0.2	0.3	-	

Table 2: Soil parameters adopted in the numerical analysis (from Miro et al. 2012).

Soil Parameters HS model		
Parameters	values	units
Friction angle, ϕ	35	[$^\circ$]
Dilatancy angle, ψ	5	[$^\circ$]
Cohesion, c	10	[kN/m^2]
Secant stiffness in the standard drained triaxial test, E_{ref}^{50}	35000	[kN/m^2]
Tangent stiffness for primary oedometer loading, E_{ref}^{oad}	35000	[kN/m^2]
Unloading and reloading stiffness, E_{ref}^{ur}	100000	[kN/m^2]
Reference pressure, p_{ref}	100	[kN/m^2]
Power for stress-level dependency of stiffness, m	0.7	[-]
Failure ratio, R_f	0.9	[-]
Poisson's ratio for unloading-reloading, ν_{ur}	0.2	[-]
Soil weight above phreatic level, γ_{unsat}	17	[kN/m^3]
Soil weight below phreatic level, γ_{sat}	20	[kN/m^3]
Strength reduction factor for interfaces in PLAXIS, R_{inter}	0.6	[-]

Table 1 summarizes the concrete parameters used in the present study. Tunnel-soil interactions were included using interface elements around the tunnel. Interfaces are composed of 12-node elements consisting of six pairs of nodes, which offer compatibility with the 6-noded triangular sides of the soil and tunnel lining elements, (Brinkgreve et al., 2013). An elasto-plastic Hardening Soil (HS) model was used to simulate the soil structure interaction at the tunnel-soil interface. An isotropic elastic model was used for the pile, pile cap, tunnel lining and tunnel boring machine shield (TBM). Zarev (2016)

stated that the advanced models like HS and HS small model are required for obtaining a realistic prediction of the deformations during shield tunnelling. Table 2 summarizes the soil properties adopted from Miro et al., 2012. According to Zarev (2016), the HS model allows for accounting the plastic collapse (isotropic hardening cap plasticity) as well as plastic shearing due to deviatoric loading with shear/frictional hardening (deviatoric yielding). For the deviatoric yielding a non-associated and for the cap plasticity an associated plastic flow rule is prescribed.

2.3 Numerical Analysis Procedure

The numerical modelling composed of three stages: initial geostatic equilibrium, application of an axial load at the pile head under the service condition and tunnel excavation. The simulation of the tunnelling process started from $Y/D = -5$ to $Y/D = +5$ (-30 m to +30 m) in the longitudinal direction (Y), as shown in Figure 4. The pile axis was located at $Y/D = 0.0$. At the second stage, an axial load of 1000 kN (calculated from static pile capacity) was applied to the pile head in order to simulate the service loading prior to the third stage, that is, tunnel excavation. In case of pile group analysis the load was 140.6 kN/m² distributed on the pile cap. After the application of loading, the tunnel excavation progress was simulated in 40 steps.

2.4 Tunnel Advancement Simulation Procedures

The progress of the TBM and the delayed installation of the lining at the tunnel periphery cause a stress release at the soil surrounding the tunnel. Hence, radial and longitudinal deformations will take place in the soil body

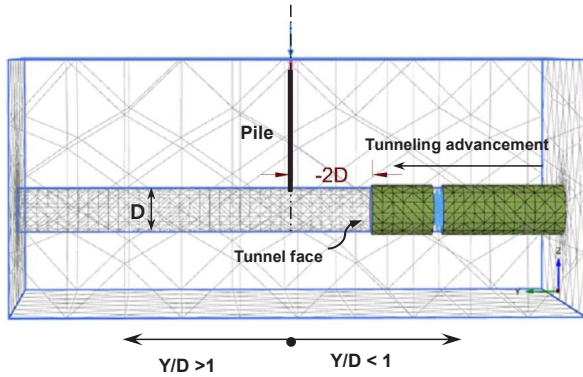


Figure 4: The zone of influence in longitudinal direction.

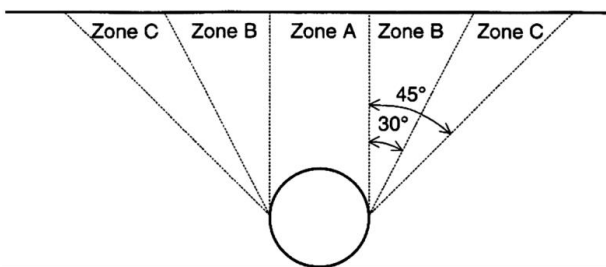


Figure 5: Zones of pile movement around a tunnel driven through soft clays and dense sands after the Heinenoord full-scale trial (Kaalberg et al. 1999).

that tends to move towards the tunnel’s cavity. This is commonly defined as (volume loss). The ground loss for a TBM excavated tunnel occurs in three stages:

- face loss (longitudinal ground movement into the tunnel face)
- shield loss (radial ground movement into the gap created by TBM overcut)
- tail loss (due to the gap closure at the tail).

Field observations showed that pile settlement could be classified into three categories, depending on the position of the pile toe relative to the tunnel axis (see Fig. 5). In particular piles with their bases in Zone A settled more than the ground surface, the piles in Zones B settled approximately by the same amount as the ground surface and the piles found in Zones C settled less than the ground surface (Kaalberg et al., 1999).

Several previous studies indicate that piles with their tips directly above the tunnel (i.e., within a horizontal offset of one tunnel radius from the tunnel axis) are likely to settle more than the surface, whereas piles outside this area generally settle less than the surface. This causes a narrowing of the pile head settlement profile with respect

to the greenfield surface settlement trough, leading to an increased potential for building damage. Moreover, assessing tunnelling induced deformations in buildings using a tunnel-pile interaction analysis (i.e. assuming that the building follows the settlement curve obtained from a tunnel-pile or tunnel-pile group analysis) does not allow inclusion of the influence of the building on the global interaction; this may be overly conservative in the cases of relatively stiff structures, as illustrated by a case study reported by Goh and Mair (2014).

2.4.1 Numerical modelling of shield tunnelling

The construction of the shield tunnel lining consists of connecting a series of concrete ring segments, of about 1.5 m long for each segment, within the TBM to form the tunnel lining and the TBM stopped to move during the lining erection. After erecting a tunnel lining ring, the boring is continued to ensure enough space to erect the next lining ring. This process is repeated until the tunnel reaches its specified location.

The lining is modelled as a linear elastic volume element and the TBM is modelled as a linear elastic plate element. The TBM causes a gap between the external diameter of the shield and the erected concrete lining which is filled with grout during the TBM advancement. The grouting process is important to lead the settlement of the soil surface to be within acceptable limits and provides stability for the surrounding soil.

The excavation process at each segment (1.5 m) of boring is modelled as follows:

- The TBM starts to excavate the soil (deactivation of the finite elements at the tunnel head)
- Support the tunnel face by applying an adverse pressure
- Activate the TBM shield, that is, of the plate elements
- Applying a back-fill grouting pressure to the back of the TBM
- Installing (activation) a new concrete lining ring

2.5 Parametric Study

2.5.1 Effect of tunnel location relative to pile and piles group in the transverse direction (x-direction)

Several tunnelling scenarios were adopted, as shown in Table 3, in terms of transverse (x-direction) tunnel location relative to the centre of the pile or group of piles. Thus analysis series I represents the case where the central axis

Table 3: Analysis series for a single and group of piles with different offset ratio (E/D)

Analysis series	Single pile					Pile group (3×3)				
	I	II	III	IV	V	VI	VII	VIII	IX	X
C/D	0.16	0.16	0.16	0.16	0.16	0.16	0.16	0.16	0.16	0.16
E/D	0	0.5	1.0	1.5	2.0	0	0.5	1.0	1.5	2.0

Table 4: Analysis series for a single and group of piles with different depth ratio (C/D).

Analysis series	Single pile					Pile group (3×3)				
	XI	XII	XIII	XIV	XV	XVI	XVII	XVIII	XIX	XX
C/D	0.16	0.5	0.75	1.0	2.0	3.0	0.16	0.5	0.75	1.0
E/D	0	0	0	0	0	0	0	0	0	0

for both the tunnel and the single pile were considered ($E/D = 0.0$), analysis series II, III, IV, and V in which the tunnel is excavated adjacent to the piles and pile groups, giving the offset ratio (E/D) of the tunnel centre to pile centre of $E/D = 0.5, 1.0, 1.5,$ and 2.0 , respectively. The depth ratio $C/D = 0.16$ for every analysis series. For each analysis the tunnel advancement (Y/D) started from $-5 Y/D$ to $+5 Y/D$ with step length = $(0.5 Y/D)$.

2.5.2 Effect of cover ratio C/D on piles

Several depth ratios C/D were considered with $E/D = 0$ remaining constant throughout the analysis. The C/D values were $0.16, 0.5, 0.75,$ and 1.0 . Table 4 summarizes the analysis series with $C/D,$ and E/D values for a single and group of piles with a constant offset ratio ($E/D = 0$).

3 Results and Discussion

Tunnelling under and adjacent to a single and a group of piles can induce movements in the piles which can alter the axial loads of the piles. The results of the 3D finite element analyses were examined in terms of the progressive changes in the pile settlements and axial loads caused by the tunnel driving, so that the pile responses to the tunnel excavation could be identified. The results are presented in the following sections.

3.1 Effect of Tunnel Advancement ($E/D = 0$) on a Single Pile

Figure 6 presents the results of the analysis I (Table 3) with $C/D = 0.16$ and $E/D = 0$, and analysis G, where (analysis G) is the Greenfield condition tunnelling analysis without pile presence. Figure 6 shows the development of normalized pile head settlement δ_{net}/δ_i (analysis I) and soil surface settlement δ_g/δ_i (analysis G) during the tunnel excavation steps ($Y/D = -5$ to $+5$). The Greenfield soil settlement (without pile) at the same pile location is also plotted in this figure, where

- δ_{net} : is the net increase in the pile head settlement due to tunnel excavation process only excluding pile settlement developed under application of the axial pile loading ($\delta_{net} = \delta - \delta_i$).
- δ : is the total pile head settlement (combined effect of service pile loading and tunnelling)
- δ_i : is the pile head settlement (1.90 mm) due to the service pile loading prior to tunnelling
- δ_g : is the soil surface settlement at the pile centre location from the Greenfield condition (analysis G) during the tunnel excavation
- Y/D : represent the normalized tunnel advancement (distance from tunnel face to pile centre)

Negative Y/D value means that the tunnelling progress is towards the pile centre, while positive Y/D means that the tunnelling passes the pile centre.

Figure 6 shows that δ_{net}/δ_i increases as the tunnel excavation proceeds. At the end of the tunnel excavation, $\delta_{g,max}/\delta_i$, and $\delta_{net,max}/\delta_i$ reach 2.31, and 2.94, respectively. The $\delta_{g,max}$ value obtained from analysis G is 4.40 mm, and $\delta_{net,max}$ from the analysis I is 5.59 mm. The maximum pile

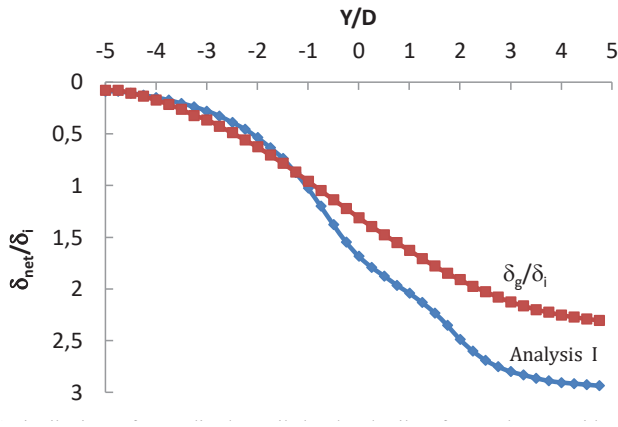


Figure 6: Distributions of normalized net pile head and soil surface settlement with tunnel advancement for single pile.

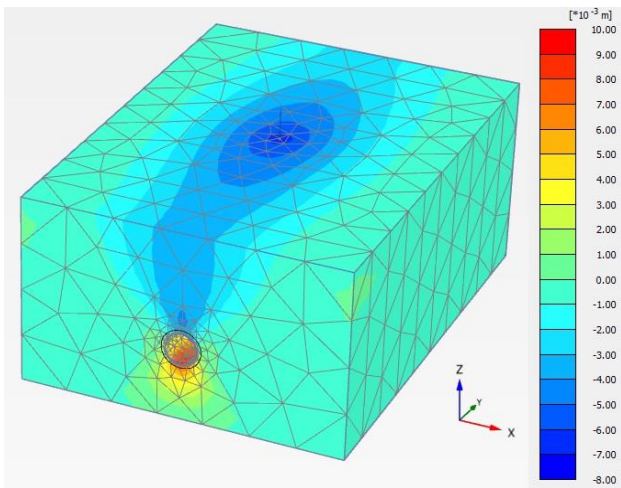


Figure 7: Displacement of soil at the end of excavation $Y/D = +5$. (Analysis I).

head settlement of the single pile due to tunnelling only is approximately 1.27 times larger than that computed from the Greenfield condition. The rate of pile settlement increases at each analysis step. Similar results were reported by Lee and Jacobsz (2006). When tunnelling was conducted within a range of $Y/D = \pm 1$, δ at $Y/D = -1$ and $Y/D = +1$ were 3.85 mm, 5.78 mm, respectively, and reaches its maximum value at the end of excavation where $\delta_{max} = 7.49$ mm, so that the percentage of settlement at $Y/D = \pm 1D$ with respect to the maximum settlement at the end of tunnel excavation (δ/δ_{max}) was approximately (51.4% to 77.2%). Similarly, when tunnelling was conducted within $Y/D = \pm 2$ from the pile centre, approximately 39 to 88.5 % of total settlement was noticed within this range. Therefore, the zone of influence on the pile head settlement in the longitudinal direction can be considered as $\pm 2D$ from the

pile centre, based on the large share of settlement that occurs within this range (about 89% of total settlement). This zone of influence is approximately close to those reported by Lee and Ng (2006), and Lee (2013). Figure 7 illustrates the soil displacement at the end of the tunnel excavation. At the end of the tunnel excavation $Y/D = +5$, the maximum pile head displacement increases by about three times relative to the initial pile head displacement.

3.2 Effect of Tunnel Advancement ($E/D = 0$) on Group of Piles

The effect of tunnel advancement on a group of piles was studied using analysis (VI) and analysis (G). Figure 8 shows the variations in the normalized pile head settlement δ_{net}/δ_i and soil surface settlement δ_g/δ_i (analysis G) for all the tunnel excavation steps ($Y/D = -5$ to $+5$), where, δ_i is the centre pile head settlement (7.85 mm) from analysis series VI due to the service pile loading prior to tunnelling.

Figure 8 shows that δ_{net}/δ_i increases as the tunnel excavation progresses. At the end of the tunnel excavation, $\delta_{g,max}/\delta_i$, and $\delta_{net,max}/\delta_i$ at the centre of the pile group were 0.56 and 0.80, respectively, the $\delta_{g,max}$ obtained from analysis G was 4.40 mm, and $\delta_{net,max}$ obtained from analysis VI for centre pile of group was 6.27 mm. The maximum head settlement of the centre pile due to tunnelling only is approximately 1.42 times that computed from the Greenfield condition. The rate of pile settlement increases at each analysis step. The results are in good agreement with Lee and Jacobsz (2006). It is clear that the longer the distance from the tunnel before reaching the pile, the smaller the pile settlement would be. When tunnelling was conducted within averages of $Y/D = \pm 1$ and $Y/D = \pm 2$ approximately 71-81% and 63-94% of total settlement was observed respectively. Therefore, the influence zone on the pile head settlement along the longitudinal direction can be considered as $\pm 2D$ from the centre of pile group, because the pile head settlement almost appeared when tunnelling was restricted from $Y/D = -2$ to $Y/D = +2$, which is in a good agreement to those reported by Lee and Ng (2006), and Lee (2013). Figure 8 shows that the centre and corner piles settlement have almost the same behaviour.

Figure 9 illustrates the displacement of soil around the piles group at the end of tunnel excavation $Y/D = +5$. The total head settlement of the centre pile was 14.12 mm (effect of service pile loading and tunnelling combined). The total pile head settlement at the end of tunnel excavation was 1.8 times the initial pile head settlement (δ_i).

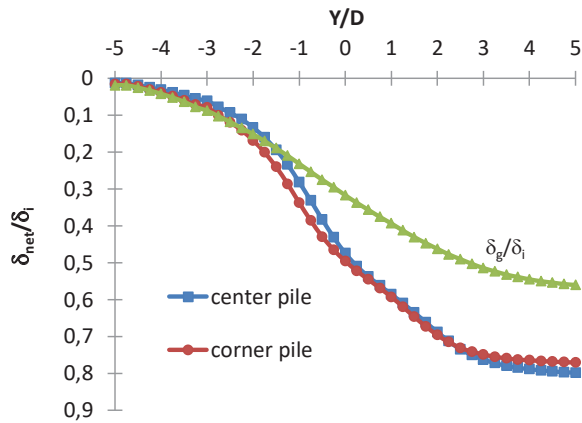


Figure 8: Distributions of normalized net pile head and soil surface settlement with tunnel advancement for group pile 3 x 3 (analysis IV and G).

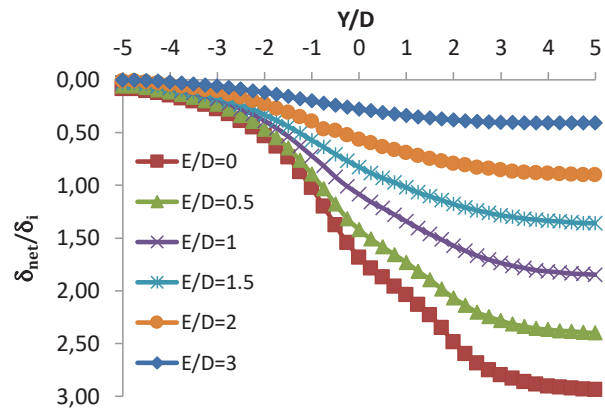


Figure 10: Variations of pile head settlement during tunnelling process for various E/D (analysis series I, II, III, IV, and V).

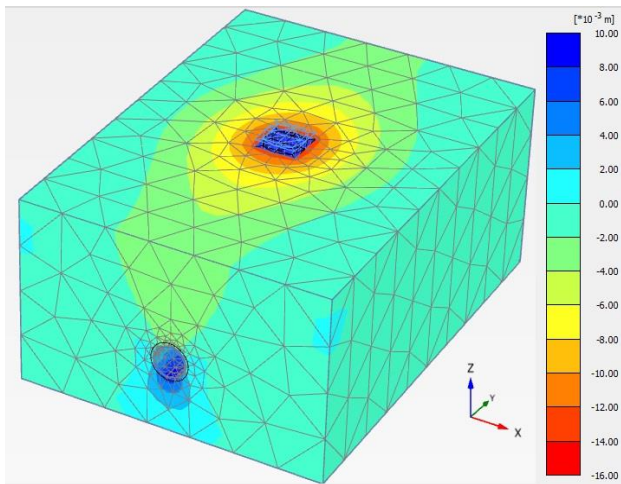


Figure 9: Soil displacement at the end of tunnel excavation Y/D= +5. (analysis VI).

3.3 Effect of Tunnel Location in Transverse X-Direction for Single Pile Analysis

The effect of transverse tunnel location relative to a pile was investigated using the pile head settlement (Table 3). Figure 10 shows the changes in the normalized net pile head settlement for the five series of analysis case, δ_{net}/δ_i for the entire tunnel excavation steps (Y/D = -5 to +5).

The value of C/D remains constant for all the five cases at 0.16. Figure 10 shows that larger distance in the transverse x-direction of the tunnel from pile results in smaller pile head settlement, which means that d_{net} at E/D = 0 is 3.25 times d_{net} at E/D = 2. From Figure 10, in case E/D = 0 the net settlement at the end of tunnel excavation is equal to 2.94 times the settlement due to service load, while in case of E/D = 2 the net settlement equal to 0.91

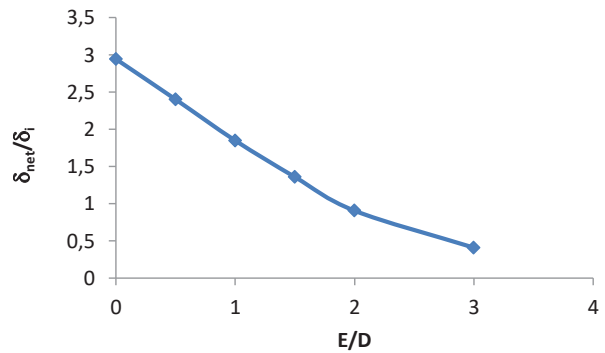


Figure 11: Variation of normalized net pile head settlement with E/D at the end of tunnel excavation (Y/D= +5).

times the settlement due to service load at the end of the tunnel excavation.

It is shown that δ_{net}/δ_i decreases with increasing the lateral distance from the tunnel to the pile. The pile head settlements at the end of the tunnel excavation obtained from Figure 10 are plotted against the lateral distance E/D as shown in Figure 11. As can be seen in this figure, δ_{net}/δ_i decreases with an increase in the lateral distance from the tunnel to the pile, and these values become small when E/D is greater than 2.0, indicating that the effect of tunnelling on piles located beyond 2D from the tunnel is not significant

3.4 Effect of Tunnel Location Relative to Pile in Transverse X-Direction for Group Piles Analysis

The effect of tunnel location relative to a group of piles is investigated using the pile head settlement as given in

Table 3. Figure 12 shows a variations in the normalized net pile head settlement (centre pile) for the five series of group piles analyses, (δ_{net}/δ_i) for the entire tunnel excavation steps ($Y/D = -5$ to $+5$), where δ_i is the centre pile head settlement (7.85 mm) due to the service pile loading prior to tunnelling. As seen in Figure 12 when $E/D=0$ the centre pile suffered the largest head settlement of $\delta_{net} = 6.27$ mm upon the completion of tunnel driving, while $\delta_{net} = 2.03$ mm at $E/D=2$. Figure 12 shows that the larger the distance in transverse X-direction of the tunnel from the centre pile the smaller the pile head settlement, which indicates that δ_{net} at $E/D=0$ is 3.07 times δ_{net} at $E/D = 2$. Figure 12 also shows that in case of $E/D = 0$ the increase in pile settlement caused by tunnelling is 80% of settlement due to service load while in case $E/D = 2$ the increase in pile head settlement caused by tunnelling is 25% of the settlement due to service load. It is evident that δ_{net}/δ_i in all cases decrease with increasing the lateral distance from the tunnel to the pile. These values are small when $E/D > 2.0$, indicating that the effect of tunnelling on the group that has its centre located beyond 2D from the tunnel may be ignored.

3.5 Effect of Tunnel-Pile Clearance, C/D on a Single Pile

The effect of Tunnel-pile clearance, C/D is examined using the pile head settlement of analyses

series shown previously in Table 3 for single pile analysis. Figure 13 shows the variations in the normalized pile head settlement δ_{net}/δ_i for all the tunnel excavation steps ($Y/D = -5$ to $+5$). It is shown that the settlement increases with increasing C/D up to the tested value of $C/D = 2$. However, all the curves of different C/D ratios coincide after $Y/D = 0$, so that once the tunnel face comes under the pile centre there would be no further increase in the settlement with tunnel progress. Therefore, it is reasonable to consider $C/D = 2$ as the limit after which the tunnelling would be safe enough.

3.6 Effect of Tunnel-Pile Clearance, C/D on Group of Piles

Table 4 also shows the analysis series that represent the group of piles cases under several ratios of (C/D). Figure 15 shows the changes in the normalized pile head settlement δ_{net}/δ_i for all these series during the tunnel excavation ($Y/D = -5$ to $+5$), where δ_i is again the centre pile head settlement (7.85 mm) due to the service pile loading prior to tunnelling.

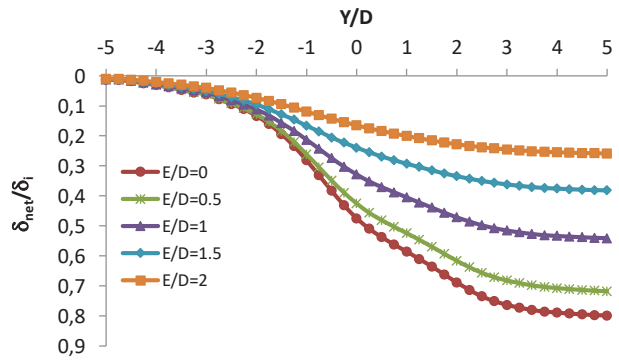


Figure 12: Variations of center pile head settlement at (3 x 3) piles group during tunnelling process for various E/D.

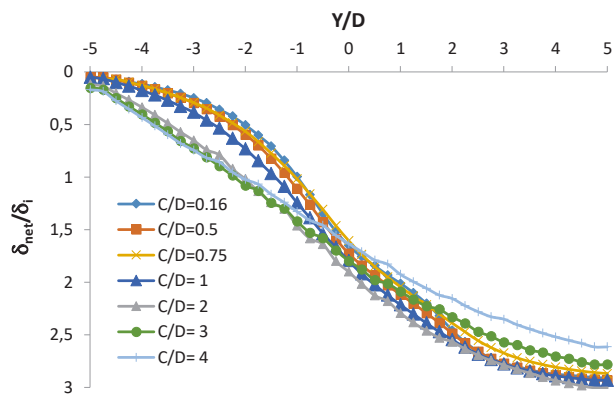


Figure 13: Distributions of normalized net pile head settlement with tunnel advancement for various C/D (single pile).

As shown in Figure 15, the net pile head settlement shows a little increase with the increase of C/D ratios until $Y/D = 0$, the case when the tunnel comes under the centre of the group; after that the settlement remains approximately constant. At $Y/D = 0$, δ_{net}/δ_i for C/D 0.16, 0.5, 0.75, and 1.0 are equal to 0.47, 0.48, 0.48, and 0.49, respectively. At $Y/D = -1$, δ_{net}/δ_i for C/D 0.16, 0.5, 0.75, and 1.0 are equal to 0.28, 0.31, 0.33, and 0.34, respectively.

It could be concluded that as the tunnel excavation progresses toward the piles group, δ_{net}/δ_i slightly increases when C/D increases, but after the tunnel passes the group δ_{net}/δ_i becomes approximately equal for all the suggested values of C/D .

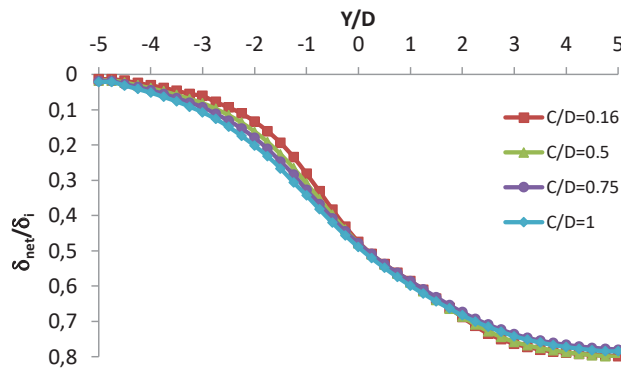


Figure 15: Distributions of normalized net pile head settlement with tunnel advancement for various C/D (group of piles). Analysis series (XV, XVI, XVII, and XVIII).

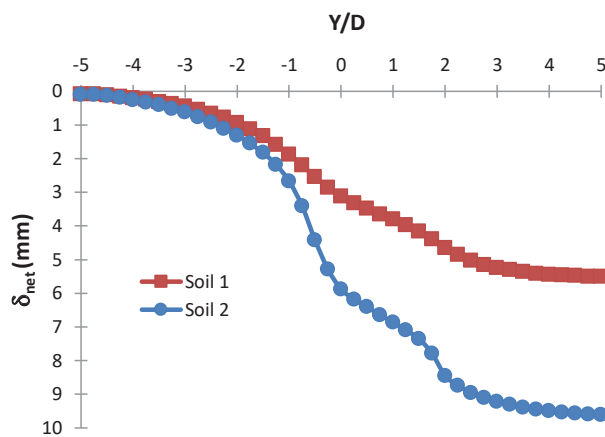


Figure 16: Distributions of net pile head settlement with tunnel advancement for two types of soils and a single pile analysis ($C/D=0.16$, and $E/D=0$).

4 The Influence of Soil Type on Pile Settlement during Tunnel Advancement

The influence of soil type on pile settlements during tunnel advancement was examined using two soil types: the first soil type was (c & ϕ) soil which is referred to as (soil 1), with the parameters shown in (Table 2). The second soil type was a sand and referred to as (soil 2) with $\phi = 37$ and cohesion = 0. Table 5 summarizes the parameters of the two types of soil. The tunnel diameter is 6 m, pile diameter is 1 m, pile length is 18 m, and a single pile was used. Analysis series I is used for both soils, $C/D = 0.16$, and $E/D = 0$.

Figure 16 shows the changes in the net pile head settlement (δ_{net}) during tunnel excavation (Y/D) for the two types of soil. The pile head settlement due to the

Table 5: Analysis series for a single and group of piles with different depth ratio (C/D).

Soil type	ϕ (degree)	c (kN/m ²)
1*	35	10
2	37	0

*Soil 1 has the same parameters as the soil used in (Table 2)

service pile loading prior to tunnelling is $\delta_i = 1.90$ mm for soil 1, while it is $\delta_i = 4.43$ mm for soil 2. This means that the sandy soil has settled more than the clay soil, which is due to the absence of the cohesion in the sandy soil. The settlement is small for both soils until reaching $Y/D = -2$. After reaching $Y/D = -2$ the settlement of soil 2 becomes larger than soil 1 but in both soils the settlement almost stabilized to a constant value of $Y/D = +2$.

Therefore, the zone of influence on the pile head settlement in the longitudinal direction is approximately the same for both types of the soil, and it can be considered as $\pm 2D$ from the pile centre, based on the large share of settlement which occurs within this range (about 89% of total settlement for soil 1, and about 92% for soil 2).

5 The Zone of Influence

According to the results presented in this paper, it may be noticed that there is a zone of significant influence underneath the pile. If the tunnel advancement is kept off this zone then there should be no fear of pile collapse based on the assumption upon which this research is accomplished. This zone involves:

1. a distance $\pm 2D$ from the pile in the longitudinal direction.
2. a distance of $\pm 2D$ from both sides of the pile in the lateral direction.
3. a zone of $2D$ vertically below the pile tip.

In conclusion, there is a virtual parallelogram as shown in Figure 17 with side dimensions of $4D \times 4D$ and $2D$ vertically with the upper surface being tangent to the pile tip and perpendicular to the pile axis. The space of this parallelogram represents the zone of significant influence during tunnel advancement below piles and it is advised to avoid this space.

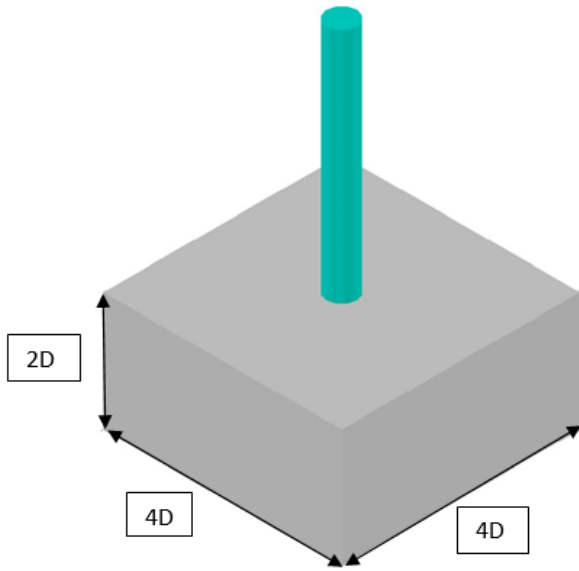


Figure 17: Virtual parallelogram represents the zone of significant influence during tunnel advancement.

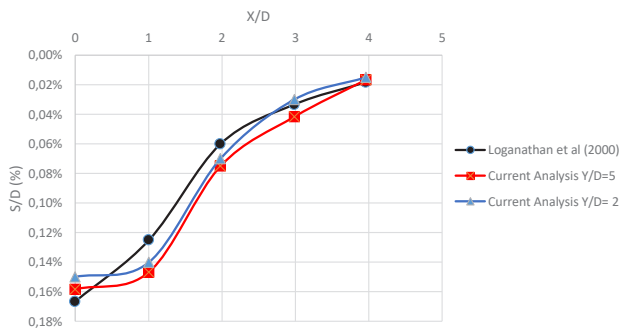


Figure 18: Comparison of the present numerical analysis with centrifuge test results.

6 Comparison with Experimental Work

Although numerical analysis is considered as an efficient tool for solving complex geotechnical problems, the results become more reliable if it compares reasonably with other experimental or field data.

A centrifuge model performed by Logagnathan et al. (2000) was adopted in this study to check the validity of the present finite element analysis using Plaxis-3D program. Logagnathan et al. (2000) performed three tests in a plain strain rigid box to investigate the effect of tunnel on the ground deformation as well as on the nearby single and group of (2 × 2) piles. The ground loss was modelled by simultaneously pulling out the soil in the annulus between

Table 6: Details of centrifuge tests (prototype scale), Logagnathan et al. (2000).

Test No.		Tunnel depth, H: m
1	Pile length, $L_p = 18$ m Pile diameter, $d = 0.8$ m	15
2	$EI = 1400$ MN m ² Tunnel diameter, $D = 6$ m	18
3	Stiff kaolin clay, ~ 75 kPa	21

the aluminium inner core and outer membrane, which cover the core along the tunnel; whereas, the volume loss was modelled progressively in the present finite element analysis. The details of the centrifuge tests are shown in Table 6.

The previous analysis illustrates that more than 89% of the settlement appeared at $Y/D = +2$ as given in section (4). Therefore this distance may be considered when assessing the tunnelling effect in when compared with Logagnathan et al. (2000). The comparison with the centrifuge test (test-3) shows reasonable agreements, as shown in Figure 18.

7 Conclusions

A series of three-dimensional parametric numerical analyses were performed to study the response of a single pile and 3 x 3 pile group to shield tunnelling in the soil. The aim of the study was to identify the fundamental governing mechanism of the response of the pile to shield tunnelling, in terms of the pile head settlements and the pile axial load. The following conclusions can be drawn from the present study:

1. Tunnelling might induce a significant increase in the net pile head settlement δ_{net}/δ_i compared to the pile head settlement induced by the application of service load. This increase may amount to 300% calculated at the end of the excavation on $Y/D = +5$ in case $E/D = 0$, $C/D = 0.16$ (where E is the lateral distance from the tunnel centre to the pile centre, C is the vertical clearance between the tunnel crown and the pile tip, and D is the tunnel diameter).
2. The influence zone on the pile head settlement along the longitudinal direction can be considered as $\pm 2D$ from the pile centre, based on the large share of settlement that occurs within this range (about 89% of total settlement for the single pile and 94% of total settlement for the centre pile in the group).

3. The pile head settlement increases with the progress of tunnel face towards the pile and continues to increase after the tunnel passes through the pile; the pile settlement increase becomes negligible at a distance equal to 5D beyond the pile.
4. The maximum pile head settlement of the single pile due to tunnelling only is 1.27 larger than that computed from the Greenfield (tunnelling analysis without pile presence condition), while for a centre pile of the group 1.42 times larger than that computed from the Greenfield condition.
5. Larger distance in the lateral x-direction of the tunnel from pile results in smaller pile head settlement, δ_{net} at $E/D = 0$ is 3.25 times δ_{net} at $E/D = 2$. The tunnelling shows the insignificant effect as it passes laterally 2D away from the piles.
6. The zone of influence in the vertical direction is limited to $C/D \leq 2$.

References

- [1] Basile, F. (2014). Effects of tunnelling on pile foundations. *Soils and Foundations*, 54(3), 280-295. DOI: 10.1016/j.sandf.2014.04.004.
- [2] Zidan, A.F. and Ramadan, O.M.O. (2015). Three dimensional numerical analysis of the effects of tunnelling near piled structures, *KSCCE Journal Civil Engineering*, 19(4), 917-928. DOI: 10.1007/s12205-014-0741-6.
- [3] Bezuijen, A. and van der Schrier, J. S. (1994). The influence of a bored tunnel on pile foundations. In Proceeding of Centrifuge 94, (pp.681-686). Balkema.
- [4] Boonsiri, I. and Takemura, J. (2015). Observation of Ground Movement with Existing Pile Groups Due to Tunneling in Sand Using Centrifuge Modelling. *Geotechnical and Geological Engineering*, 33(3), 621-640. DOI: 10.1007/s10706-015-9845-0.
- [5] Bowles, J. E. (1997). *Foundation Analysis and Design* (5th ed). McGraw-Hill Companies, Inc.
- [6] Brinkgreve, R. B. J. Engin, E. and Swolfs, W. M. (2013) eds, Plaxis 3D tutorial manual.
- [7] Chapman, D., Metje, N., Stärk, A. (2010). *Introduction to Tunnel Construction* (2nd ed). CRC Press, Taylor & Francis Group.
- [8] Fattah, M. Y., Shlash, K. T. & Al-Soud, M. S. (2012). Boundary Element Analysis of a Lined Tunnel Problem. *International Journal of Engineering*, IJE TRANSACTIONS B: Applications Vol. 25, No. 2, (May 2012), pp.87-94.
- [9] Forth, R. A., & Thorley, C. B. B. (1996). Hong Kong Island line predictions and performance. In Proceeding of the International Symposium on Geotechnical Aspects of Underground Construction in Soft Ground (pp.677-682), London, Balkema.
- [10] Goh, K.H. & Mair, R.J. (2014). Response of framed buildings to excavation-induced movements. *Soils and Foundations*, 54 (3), 250–268.
- [11] Hergarden, H. J. A. M., Van der Poel, J. T. & Van der Schrier, J. S. (1996). Ground movements due to tunnelling: Influence on pile foundations. In Proceedings of the International Symposium on Geotechnical Aspects of Underground Construction in Soft Ground, April 15-17 (pp.519-524), London. R. J. Mair & R. N. Taylor (eds).
- [12] Jacobsz, S. W., Standing, J. R., Mair, R. J. Hagiwara, T. & Sugiyama, T. (2004). Centrifuge modeling of tunneling near driven piles. *Soils & Foundations*, 44(1) 49-56. DOI: 10.3208/sandf.44.49.
- [13] Kaalberg, F. J. Lengkeek, H. J. and Teunissen, E.A.H. (1999), "Evaluatie van de meetresultaten van het proefpaleproject ter plaatse van de tweede Heinenoord tunnel" (in Dutch), Adviesbureau Noord/Zuidlijn, Amsterdam (No. R981382).
- [14] Lee, C.J. (2012). Three-dimensional numerical analyses of the response of a single pile and pile groups to tunnelling in weak weathered rock. *Tunnelling and Underground Space Technology*, (32), 132–142. DOI: 10.1016/j.tust.2012.06.005.
- [15] Lee, C.J. (2013). Numerical analysis of pile response to open face tunneling in stiff clay. *Computers and Geotechnics*, (51), 116–127. DOI: 10.1016/j.compgeo.2013.02.007.
- [16] Lee, C.J. & Jacobsz, S.W. (2006). The Influence of Tunnelling on Adjacent Piled Foundations. *Tunnelling and Underground Space Technology*, 21 (3–4), 430-435. DOI: 10.1016/j.tust.2005.12.072.
- [17] Lee, G.T.K. and Ng, C.W.W. (2006). Three-dimensional numerical simulation of tunnelling effects on an existing pile. In K.J. Bakker, A. Bezuijen, W. Broere, and E.A. Kwast (eds) *Geotechnical Aspects of Underground Construction in Soft Ground* (pp. 139-144). London: Taylor & Francis Group.
- [18] Lee, C.J. Jun, S.H. Yoo, N.J. & Kim, G.W. (2007). The effects of tunnelling on an adjacent single pile. In Barták, J., Hrdina, I, Romancov, G. & Zlámal, J. (eds), *Underground Space – the 4th Dimension of Metropolises* (pp. 527-532). London, Taylor and Francis Group.
- [19] Lee, C.J. Jeon, Y.J. Kim, S.H. and Park, I.J. (2016). The influence of tunneling on pre-existing piled foundation in weathered soil. *Geomechanics and Engineering*, 11(4), 553-570. DOI: 10.12989/gae.2016.11.4.553
- [20] Loganathan, N. Poulos, H. G. & Stewart, D. P. (2000). Centrifuge model testing of tunnelling-induced ground and pile deformations. *Geotechnique*, 50(3), 283–294. DOI: 10.1680/geot.2000.50.3.283.
- [21] Mair, R. J. (1993). Developments in geotechnical engineering research: Application to tunnels and deep excavations. In Proceedings of the Institution of Civil Engineers, Civil Engineering, February 1993. 97(1), 27–41.
- [22] Mair, R. & Williamson, M. (2014). The influence of tunnelling and deep excavation on piled foundations. In Proceedings of the 8th International Symposium on Geotechnical Aspects of Underground Construction in Soft Ground, 25-27 August 2014 (pp. 21-30). Seoul, South Korea, C., Park, S.-W., Kim, B., Ban, H. (Eds.), Taylor and Francis.
- [23] Miro, S., Hartmann, D., Schanz, T., & Zarev, V. (2012). System Identification Methods for Ground Models in Mechanized Tunneling. In 19th International Conference on the Application of Computer Science and Mathematics in Architecture and Civil Engineering, 4-6 July 2012. University Weimar, Germany. K. Gürlebeck, T. Lahmer and F. Werner (eds.)

- [24] Mazek, S.A. (2014). Evaluation of surface displacement equation due to tunneling in cohesionless soil. *Geomechanics and Engineering*, 7(1), 55-73. DOI: 10.12989/gae.2014.7.1.055.
- [25] Ng, C.W.W., Lu, H. and Peng, S.Y. (2013). Three-dimensional centrifuge modelling of the effects of twin tunnelling on an existing pile. *Tunnelling and Underground Space Technology*, (43), 350-361. DOI: 10.1016/j.tust.2012.07.008.
- [26] Zarev, V. (2016). *Model identification for the adaption of numerical simulation models – Application to mechanized shield tunneling*. Ph.D. Dissertation, Ruhr University, Bochum, Germany.
- [27] Yang, M., Sun, Q., L., MA K. (2011). Three-Dimensional Finite Element Analysis on Effects of Tunnel Construction on nearby Pile Foundation. *Journal of Central South University of Technology*. 18(3), 909-916. DOI: 10.1007/s11771-011-0780-9.
- [28] Yoo, C. (2013). Interaction between Tunneling and Bridge Foundation a 3D Numerical Investigation. *Computers and Geotechnics*. (49), 70–78. DOI: 10.1016/compgeo.2012.11.005.